

Metallicity

Where do metals come from?

What controls the metallicity of a galaxy?

How do we measure it?

Results.

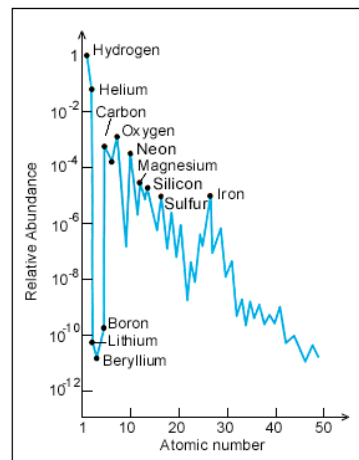
1

Abundance: Gas Phase

The gas phase abundance of an element X is defined:

$$12 + \log(X/H)$$

of atoms



Why 12? In 1929 Henry Norris

Russell arbitrarily chose $\log(N(H)) = 12$

3

Fast terminology

"Metallicity"

For stars, usually refers to Fe

For gas, usually refers to O

Sometimes refers to all metals

X = mass fraction of Hydrogen

Y = mass fraction of Helium

Z = mass fraction of metals

"Abundance"

Usually refers to arbitrary elements

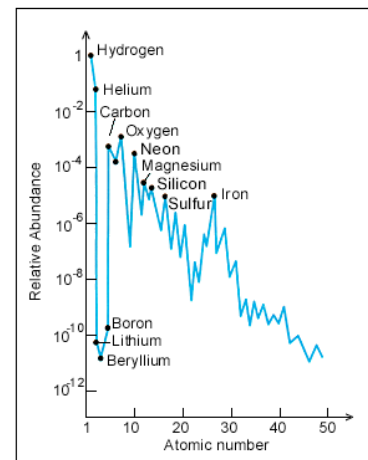
2

Abundance: Stars

Metal abundances in stars are defined relative to solar:

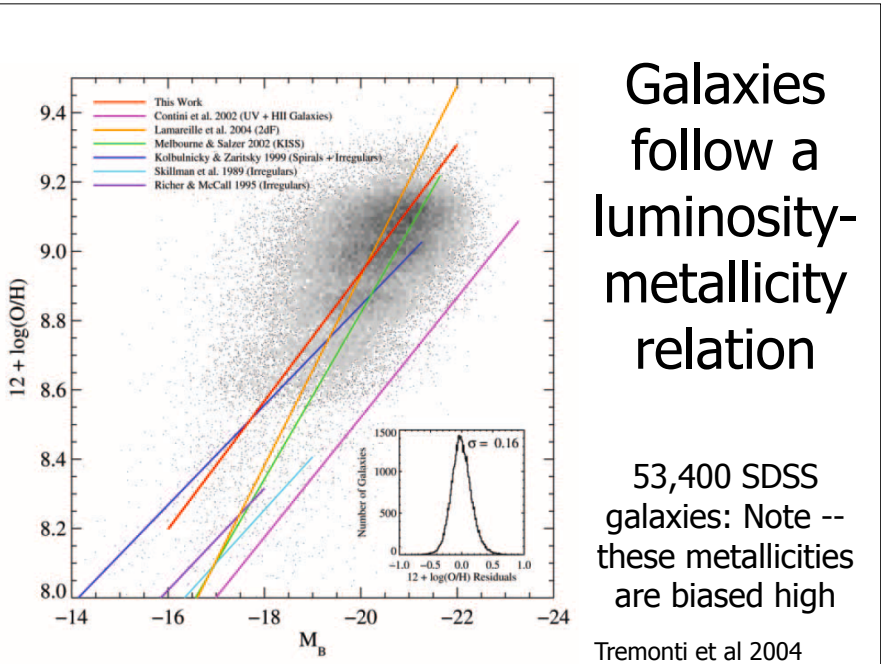
$$[\text{Fe}/\text{H}] = \log_{10} \left(\frac{N_{\text{Fe}}}{N_{\text{H}}} \right)_{\text{star}} - \log_{10} \left(\frac{N_{\text{Fe}}}{N_{\text{H}}} \right)_{\text{sun}}$$

of atoms



Can use any other species for "Fe" or "H" (i.e. [O/H], [O/Fe], etc)

4



Galaxies follow a luminosity-metallicity relation

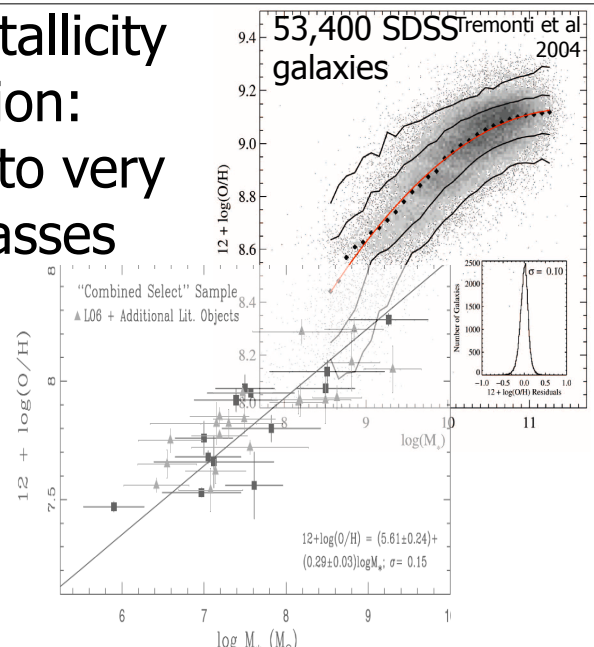
53,400 SDSS galaxies: Note -- these metallicities are biased high

Tremonti et al 2004

Mass-Metallicity Relation:
Extends to very low masses

Berg et al 2012
Weak-line “gold standard” metallicities

6

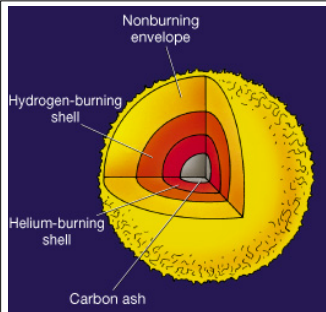


Two Ingredients Needed:

Where do metals come from?

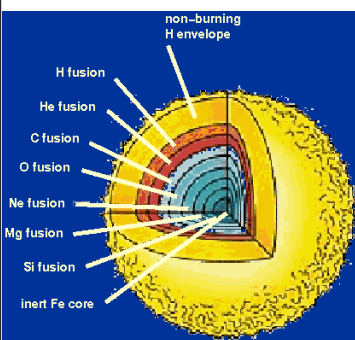
What “chemical evolution” sets the observed metallicity of a galaxy

Main Nucleosynthetic Channels
Stellar interior processing

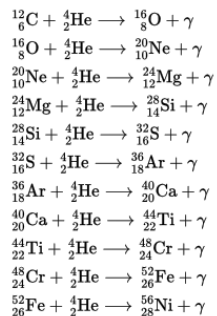


Nucleosynthesis in Stars

Low mass stars:
C or C+O core fuses up
to Fe-peak when ignites



High mass
stars:
 α -elements
through
“ α -ladder”



Main Nucleosynthetic Channels

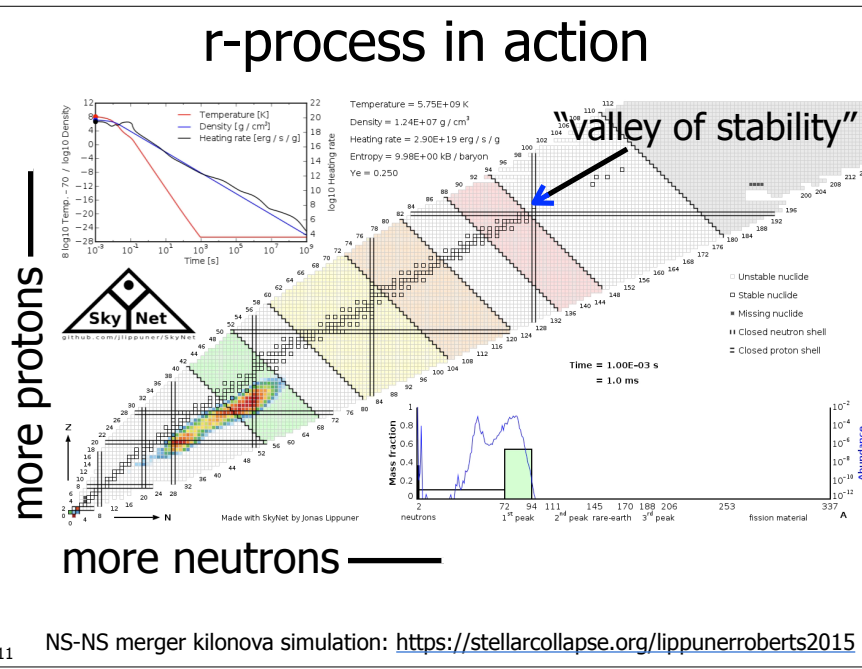
Stellar interior processing

“r-process” due to rapid accretion of neutrons, followed by subsequent β -decay to stable nuclei (starts w/ Fe)

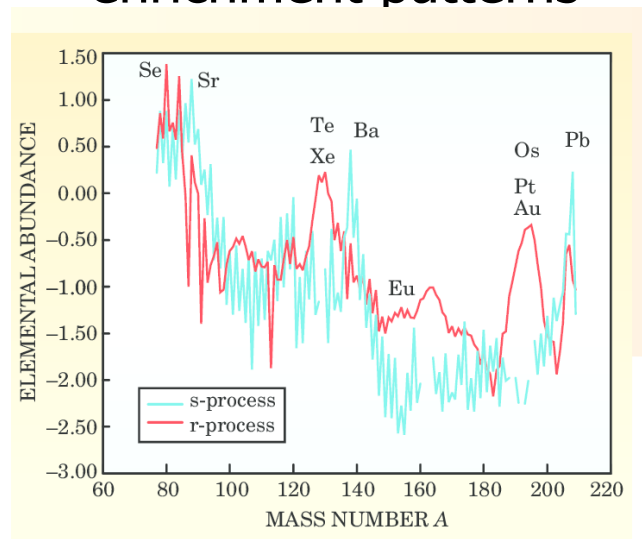
“s-process” due to slow accretion of neutrons interspersed with decay to stable nuclei (starts w/ Fe)

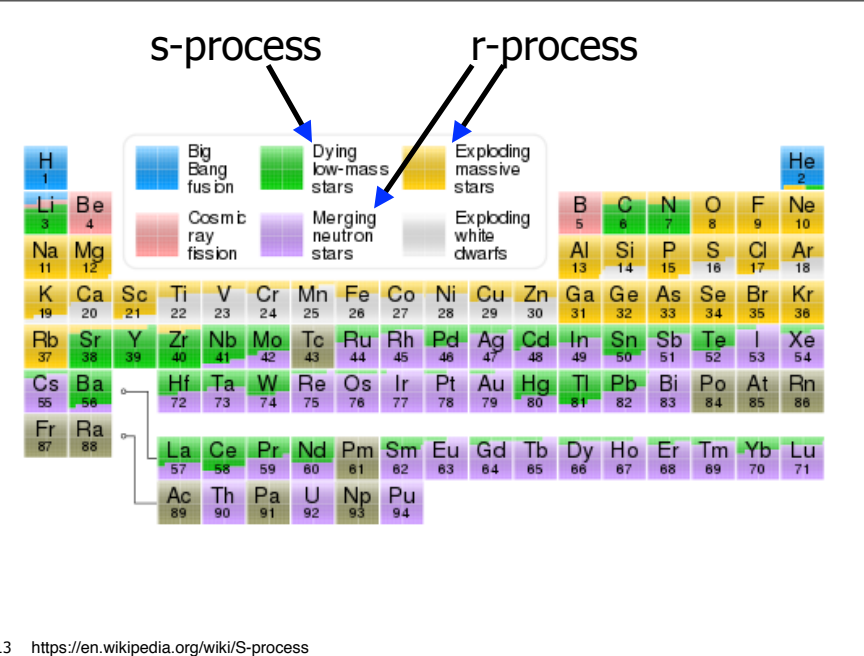
Cosmic ray spallation (induces fission)

10



r- and s-process produce different enrichment patterns





13 <https://en.wikipedia.org/wiki/S-process>

Production of Elements I.

Type II SNe ($M > 6\text{-}8 M_{\odot}$)

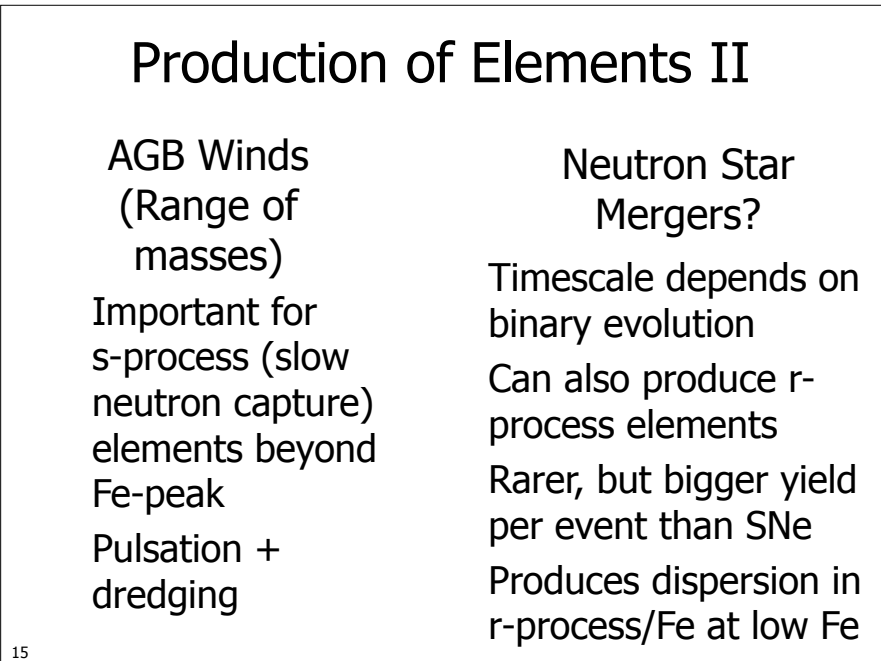
Fast enrichment
(<50 Myrs)

α -element enhanced
compared to solar
(O, Ne, Mg, Si, S, Ar,
Ca, Ti, Cr)

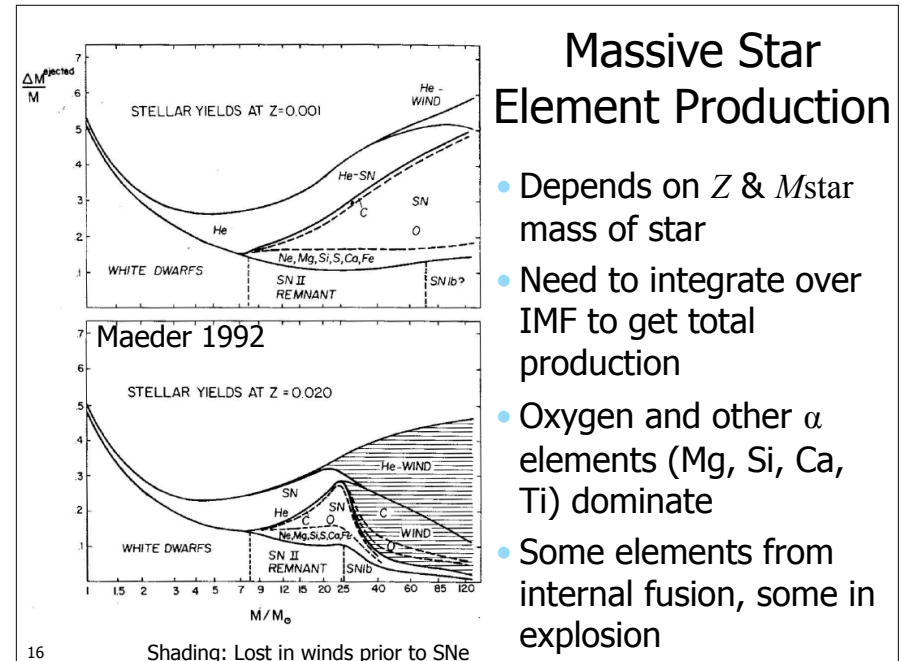
Type Ia SNe (Range of masses)

Some prompt, but
most delayed
Fe-peak elements
are dominant
products

Both produce r-process elements beyond iron peak



15



16

Shading: Lost in winds prior to SNe

Exact Type II yield is uncertain

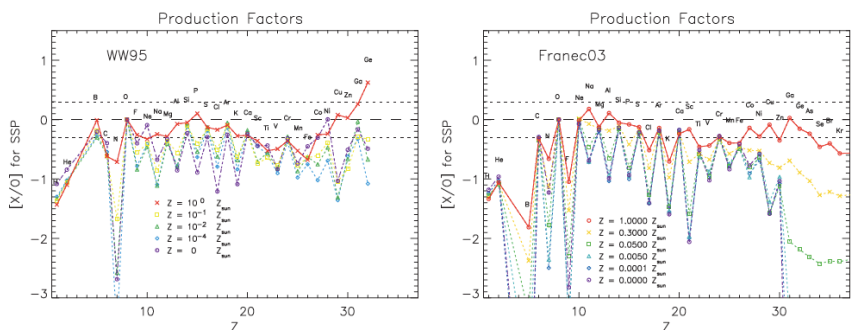


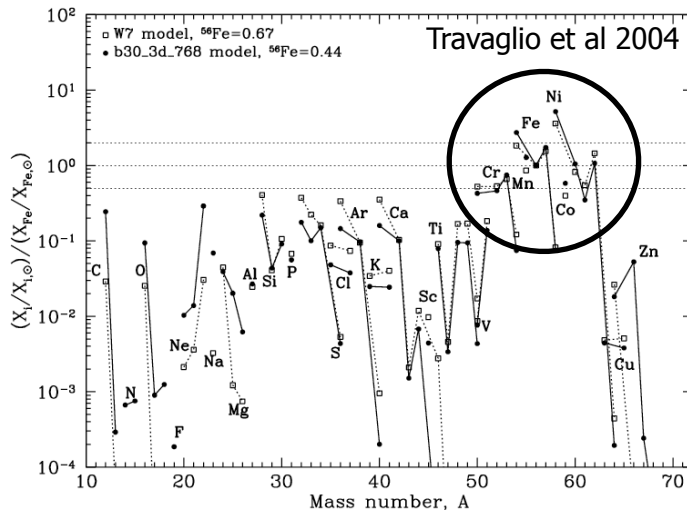
Figure 1 Production factors relative to O on a solar logarithmic scale from a single generation of massive stars using the metallicity-dependent yields of Woosley & Weaver 1995 (left panel) and those of FRANEC 2003 (right panel). The latter were kindly provided by A. Chieffi (2003, personal communication). Yields were integrated over a Salpeter (1955) IMF from 12 to 40 M_⊙. The dashed line indicates the solar values (where log(N_i/N_H)_⊙ + 12 = 8.73, Holweger 2001) and dotted lines indicate deviations from scaled solar by a factor of two. For both sets of yields C, N, and some of the iron-peak elements are subsolar because they require additional sources such as lower mass stars and Type Ia SNe. The strength of the ‘odd-even’ effect increases with decreasing metallicity in both cases, however the effect is more pronounced for FRANEC 2003.

Depends on nucleosynthetic models, metallicity, IMF

From review by Gibson et al 2003

17

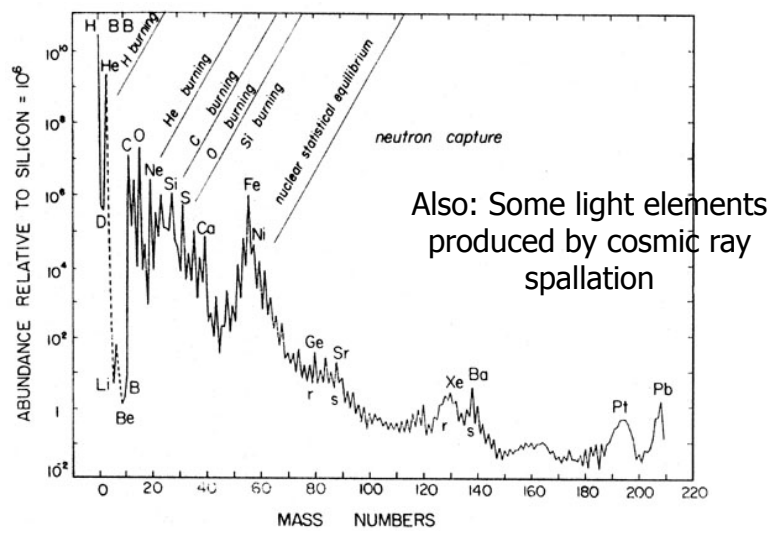
Type Ia Yields: Primarily Iron Peak



Note: Explosion models uncertain

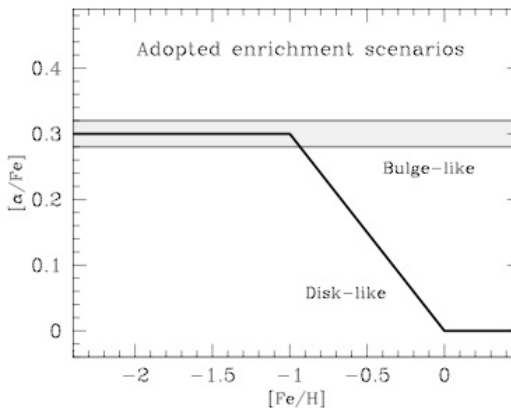
18

Solar abundance is combination of Type II, Type Ia, and s-process



19

Enrichment patterns



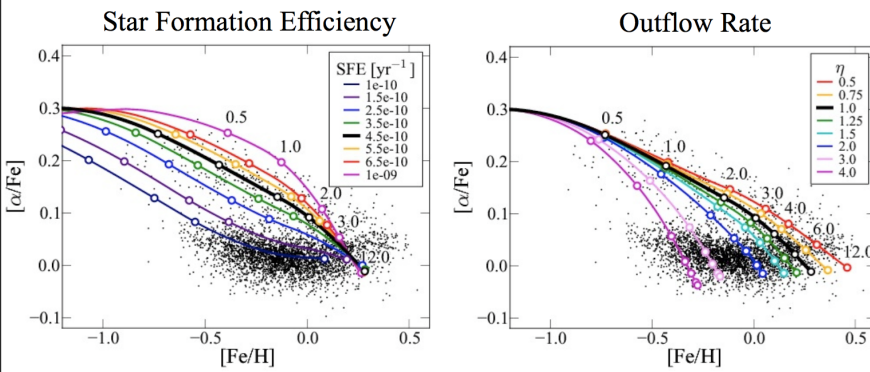
Fast enrichment:
no time for Type Ia,
so only Type II
products

Slow enrichment:
Extended SF history
allows enrichment
of Type II iron peak
elements

FIG. 1.—Sketched diagram of the [α/Fe] vs. [Fe/H] trend in the disk-/bulge-like enrichment scenarios, as adopted in our computational routine.

20

Galaxy history affects patterns



21

Andrews et al 2015 (in prep)

Application: Stars in Milky Way

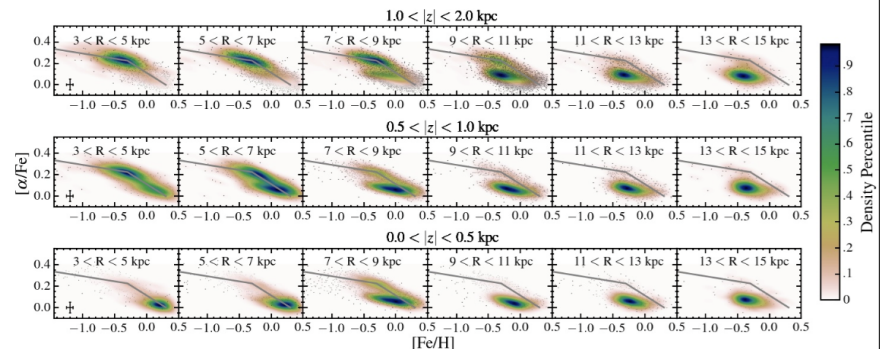


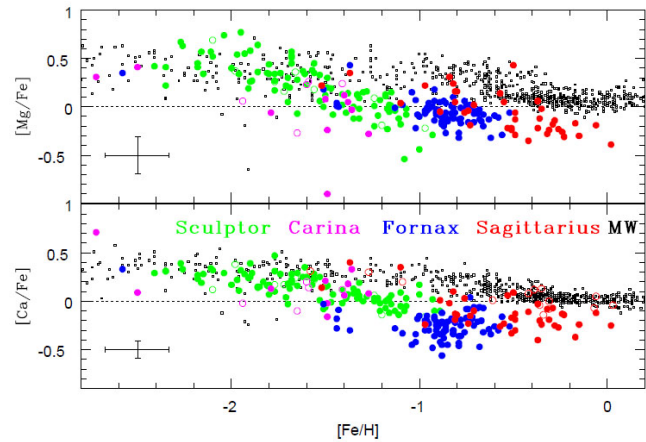
Figure 4. The stellar distribution of stars in the $[\alpha/\text{Fe}]$ vs. $[\text{Fe}/\text{H}]$ plane as a function of R and $|z|$. Top: The observed $[\alpha/\text{Fe}]$ vs. $[\text{Fe}/\text{H}]$ distribution for stars with $1.0 < |z| < 2.0$ kpc. Middle: The observed $[\alpha/\text{Fe}]$ vs. $[\text{Fe}/\text{H}]$ distribution for stars with $0.5 < |z| < 1.0$ kpc. Bottom: The observed $[\alpha/\text{Fe}]$ vs. $[\text{Fe}/\text{H}]$ distribution for stars with $0.0 < |z| < 0.5$ kpc. The grey line on each panel is the same, showing the similarity of the shape of the high- $[\alpha/\text{Fe}]$ sequence with R . The extended solar- $[\alpha/\text{Fe}]$ sequence observed in the solar neighborhood is not present in the inner disk ($R < 5$ kpc), where a single sequence starting at high- $[\alpha/\text{Fe}]$ and low metallicity and ending at solar- $[\alpha/\text{Fe}]$ and high metallicity fits our observations. In the outer disk ($R > 11$ kpc), there are very few high- $[\alpha/\text{Fe}]$ stars.

APOGEE: Higher α -enhancement above the plane, and towards the center of the galaxy. Faster SF.

22

Hayden et al 2015

Application: Stars in dwarfs

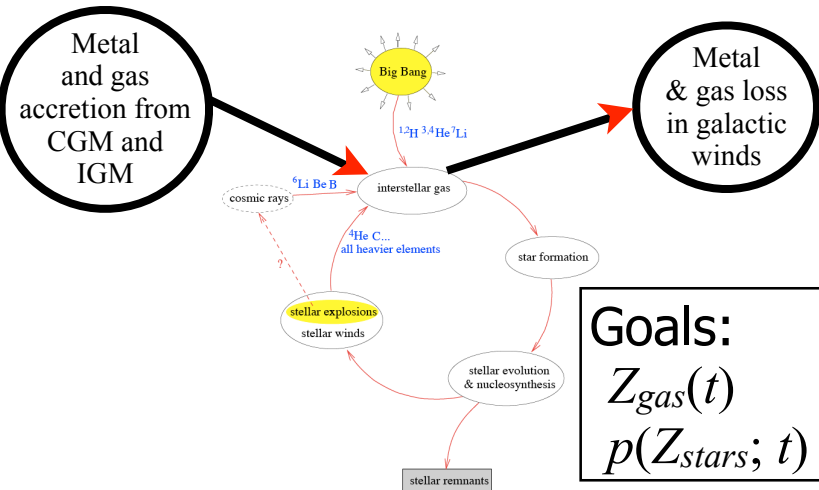


Dwarfs: Fe enrichment does not progress as far before SN II α -enhancement becomes diluted. Winds?

Venn et al 2004

What sets galaxy metallicity?

“Chemical Evolution”



24

Complex accounting problem

Masses

M_g : Total mass of interstellar gas
 M_s : Total mass of stars
 M_w : Total mass of stellar remnants (white dwarfs)
 M_t : Total mass of the system
 $M_t = M_g + M_s + M_w$

Rates

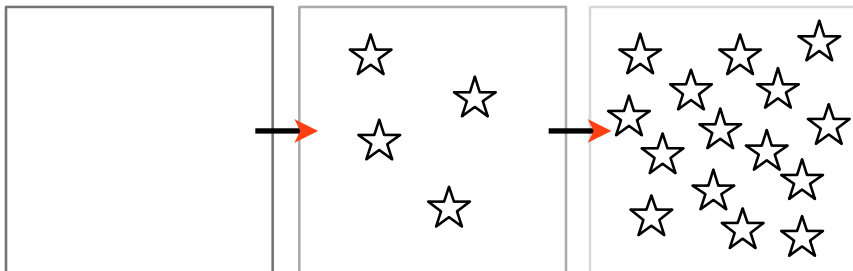
E : the rate of mass ejection from stars
 E_Z : the rate of metal ejection from stars
 W : the creation rate of stellar remnants.
 Ψ : Rate of star formation
 f : Rate of infall or outflow of material from the system
 Z_f : Metal abundance of the infall (or outflow) material
 $\phi(m)$: the Initial Mass Function

Stellar Evolution & Nucleosynthesis

Classic references: Tinsley 1980 (Fundamentals of Cosmic Physics)
Pagel 1997 (Textbook)

25

Simplest Form: “Closed Box”



$$Z_{\text{gas}} = 0$$

$$f_{\text{gas}} = 1$$

No infall or outflow

Assume “instantaneous recycling” for massive stars

Searle & Sargent 1972

Key, unfamiliar quantities:

Return Fraction (R)

The mass fraction of a generation of stars that is returned to the ISM.
Depends on time, but typically 0.2-0.3

Lock up fraction ($\alpha = 1-R$)

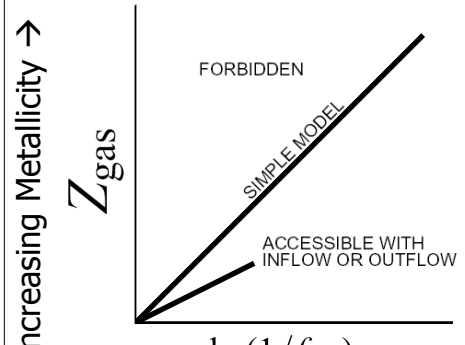
The mass fraction of a generation of stars that is locked up in long-lived stars or remnants.

“Nucleosynthetic yield” (y or p)

26

The mass in newly formed elements ejected by a generation of stars, in units of the mass locked up in long-lived stars and stellar remnants

Closed Box Model



$$Z = y_Z \ln(\mu^{-1})$$

Nucleosynthetic “yield”

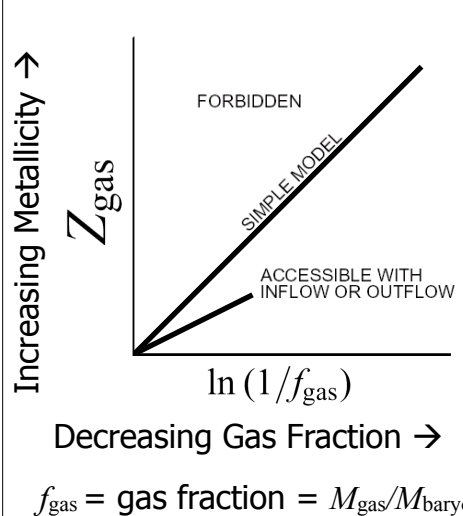
$$y_{\text{eff}} = \frac{Z(\text{obs})}{\ln(\mu^{-1})}$$

“Effective Yield”

$f_{\text{gas}} = \text{gas fraction} = M_{\text{gas}}/M_{\text{baryon}}$

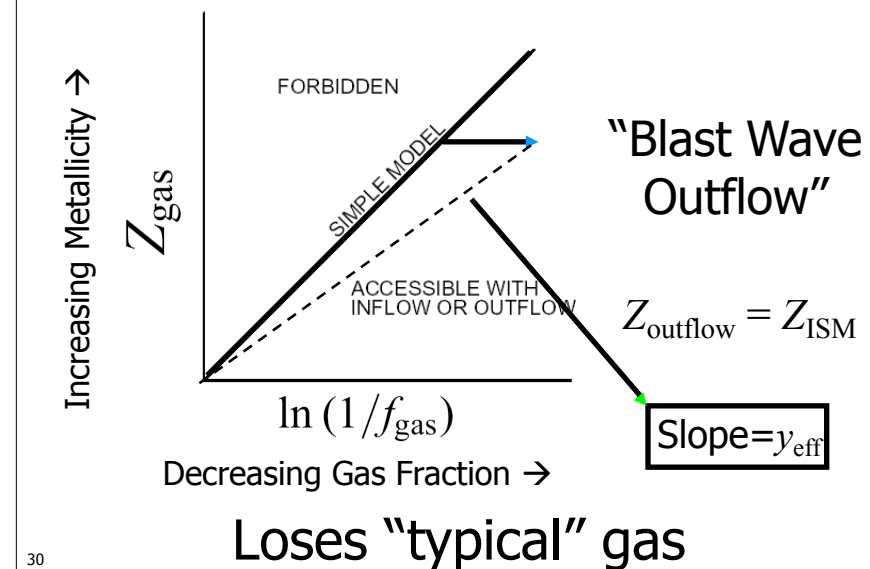
28 Edmunds 1990

If $y_{\text{eff}} \sim y_Z$, evolved like "closed box"

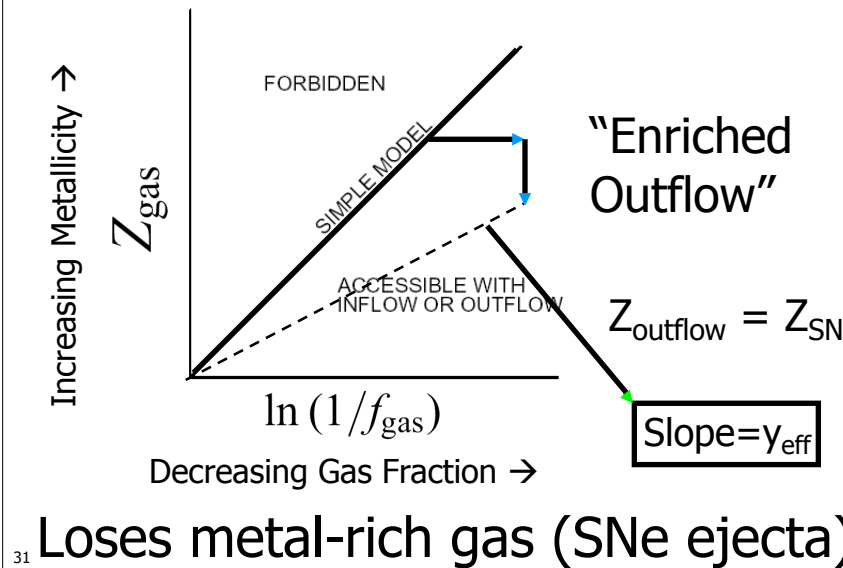


²⁹ Edmunds 1990

Deviations from closed box

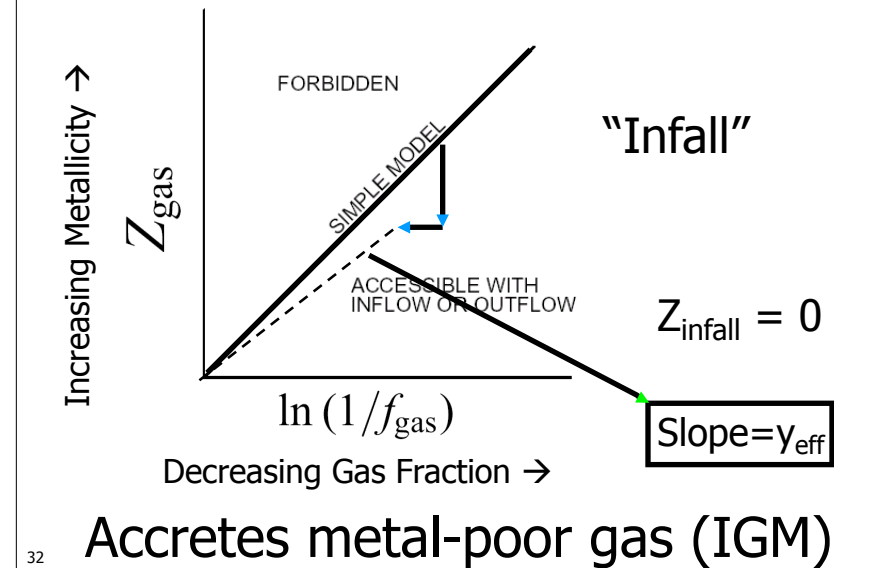


Deviations from closed box



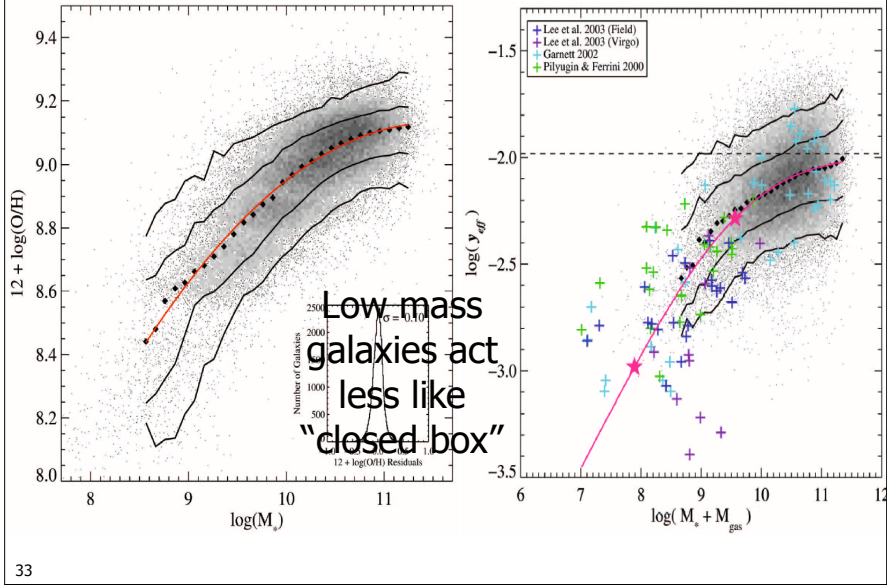
³¹ Loses metal-rich gas (SNe ejecta)

Deviations from closed box

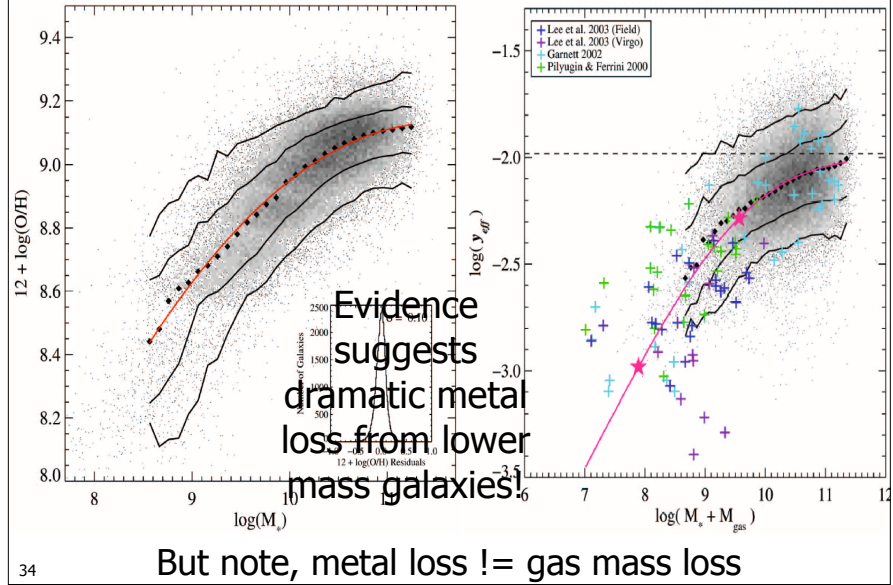


³² Accretes metal-poor gas (IGM)

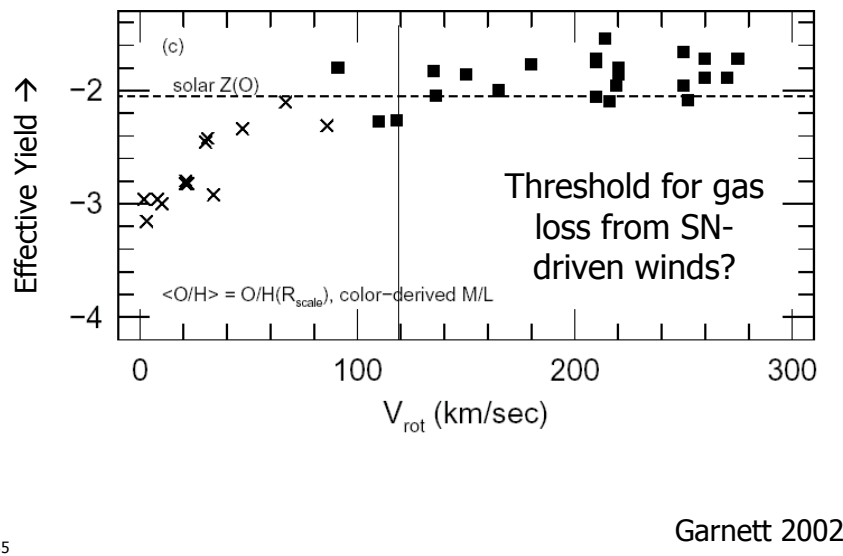
Mass-Metallicity vs Effective Yield



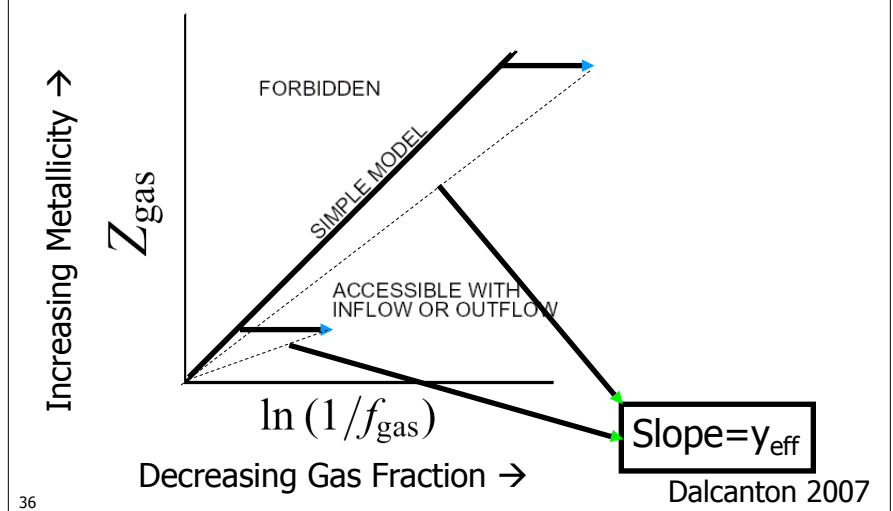
Mass-Metallicity vs Effective Yield



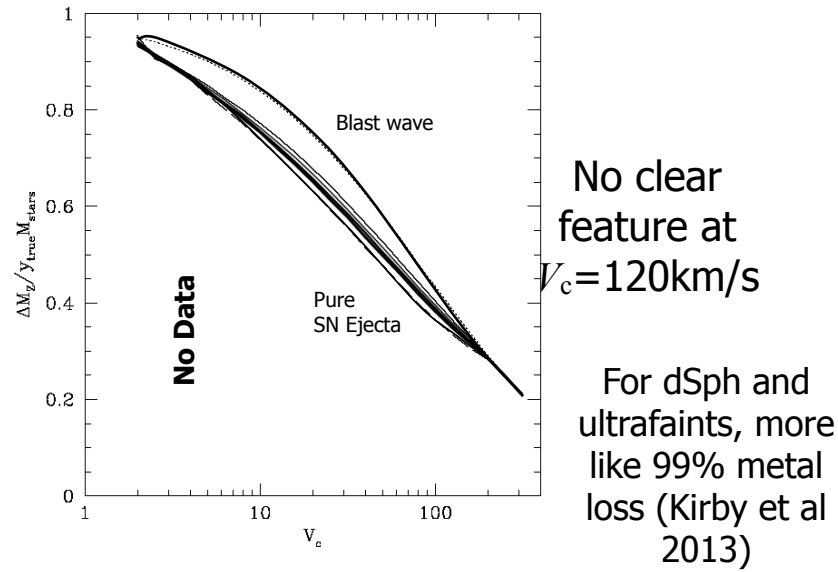
Effective yield is constant for $V > 120$ km/s



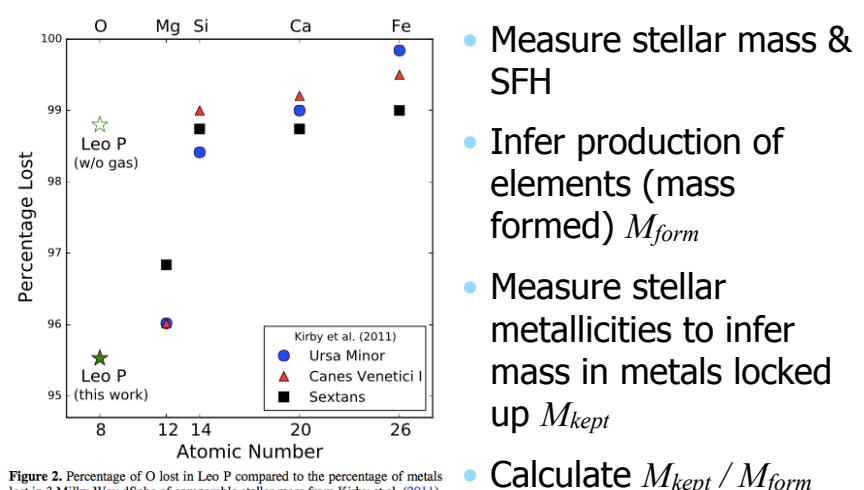
No. It's just hard to change effective yield of gas poor systems



Inferred metal loss is high, increases steadily



In LG dwarfs metal loss is near total



McQuinn et al 2015

Metallicity-sensitive indicators

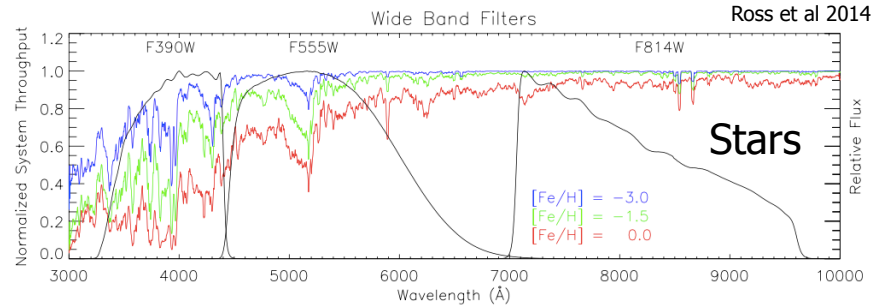
Stars:

Tracks [Fe/H] at time luminosity-weighted stellar population formed

- Broadband colors — particularly NIR
- Spectral fitting (i.e. fit template to whole spectrum).
- Equivalent widths of specific spectral features (in absorption)

39

More Metals = More absorption



More absorption lines in the blue

Redder = More metal rich

But, age effects in composite populations

Colors more robust metallicity indicator in NIR, but spectral fitting more robust in optical

40

"Age-Metallicity Degeneracy"

Ross et al 2014

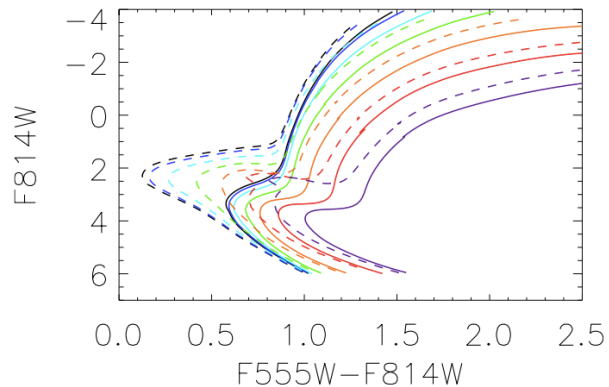


Figure 2. Age–metallicity degeneracy is shown here with isochrones of different ages covering a range of metallicity $-2.5 < [\text{Fe}/\text{H}] < +0.5$; black represents the most metal-poor, purple the most metal-rich, with each color in between representing a 0.5 increment in $[\text{Fe}/\text{H}]$; the solid lines represent an age of 12.5 Gyr and the dashed lines represent 4 Gyr.

41

Combine colors
to interpret age
& metallicity

Lines of constant
metallicity (red) have
nearly constant $J-K_s$
colors.

Lines of constant age
(green) have relatively
constant $B-V$ colors

Galaz et al 2002

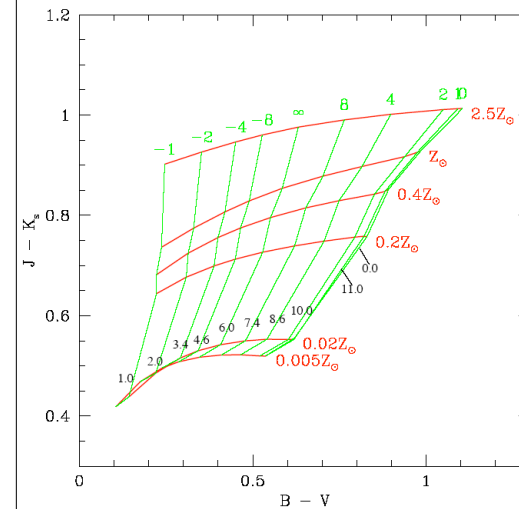
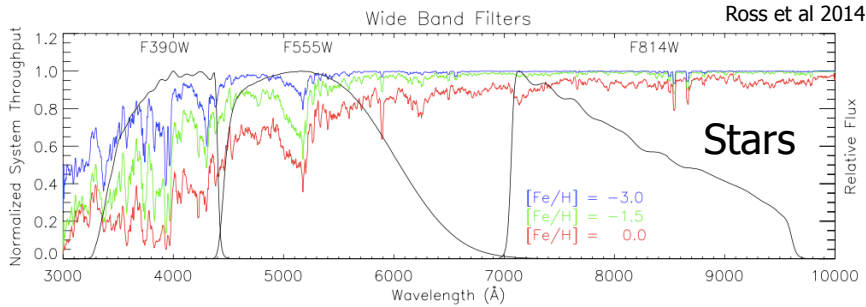


Fig. 15.— Color grid for the $J - K_s$ index as a function of the $B - V$ index, for different stellar formation rates and metallicities. Metallicities range from $0.005Z_\odot$ to $2.5Z_\odot$. Top labels denote different exponential star-formation rates, where ∞ denotes a constant star-formation rate. Bottom labels denote mean ages in Gyr. The star-formation started 12 Gyr ago for all bursts.

Caveat



Stellar metallicity indicators are light-weighted
Different galaxies will have different age stars
dominating light-weighted spectrum
Comparing stellar metallicity is not tracking
identical age across galaxies.

Caveat: Color also depends on abundance patterns

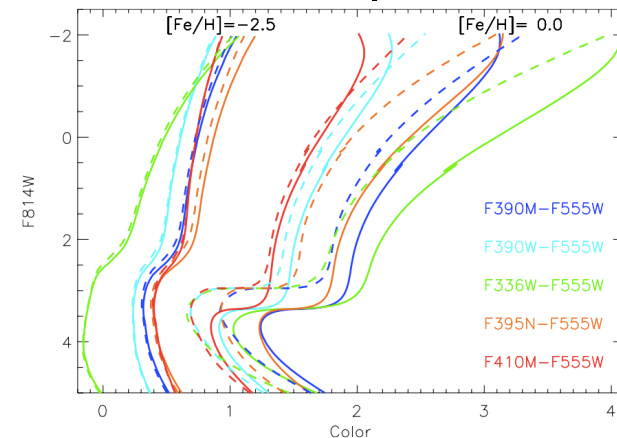


Figure 7. Color changes due to shifts in α at low and high metallicity for five metallicity-sensitive colors listed. The solid and dashed lines represent $[\alpha/\text{Fe}] = +0.4$ and 0.0 at $[\text{Fe}/\text{H}] = -2.5$, and $[\alpha/\text{Fe}] = +0.2$ and -0.2 at $[\text{Fe}/\text{H}] = 0.0$.

44

Ross et al 2014

| INDEX DEFINITIONS | | | | |
|---------------------|-----------------------|--|--------------|-------------------|
| Name (2) | Index Bandpass (3) | Pseudocontinuum (4) | Units (5) | Measures* (6) |
| CN ₁ | 4142.125–4177.125 | 4080.125–4117.625 4244.125–4284.125 | mag | C, N, (O) |
| CN ₂ | 4142.125–4177.125 | 4083.875–4096.375 4244.125–4284.125 | mag | C, N, (O) |
| Ca4227 | 4222.250–4234.750 | 4211.000–4219.750 4241.000–4251.000 | Å | Ca, (C) |
| G4300 | 4281.375–4316.375 | 4266.375–4282.625 4318.875–4335.125 | Å | C, (O) |
| Fe4383 | 4369.125–4420.375 | 4359.125–4370.375 4442.875–4455.375 | Å | Fe, C, (Mg) |
| Ca4455 | 4452.125–4474.625 | 4445.875–4454.625 4477.125–4492.125 | Å | (Fe), C, Cr |
| Fe4531 | 4514.250–4559.250 | 4504.250–4514.250 4560.500–4579.250 | Å | Ti, (Si) |
| C ₄ 4668 | 4634.000–4720.250 | 4611.500–4630.250 4742.750–4756.500 | Å | C, (O), (Si) |
| H β | 4847.875–4876.625 | 4827.875–4847.875 4876.625–4891.625 | Å | H β , (Mg) |
| Fe5015 | 4977.750–5054.000 | 4946.500–4977.750 5054.000–5065.250 | Å | (Mg), Ti, Fe |
| Mg ₁ | 5069.125–5134.125 | 4895.125–4957.625 5301.125–5366.125 | mag | C, Mg, (O), (Fe) |
| Mg ₂ | 5154.125–5196.625 | 4895.125–4957.625 5301.125–5366.125 | mag | Mg, C, (Fe), (O) |
| Mg _b | 5160.125–5192.625 | 5142.625–5161.375 5191.375–5208.150 | Å | Mg, (C), (Cr) |
| Fe5270 | 5245.650–5285.650 | 5233.150–5248.150 5285.650–5318.150 | Å | Fe, C, (Mg) |
| Fe5335 | 5312.125–5352.125 | 5304.625–5315.875 5353.375–5363.375 | Å | Fe, (C), (Mg), Cr |
| Fe5406 | 5387.500–5415.000 | 5376.250–5387.500 5415.000–5425.000 | Å | Fe |
| Fe5709 | 5696.625–5720.375 | 5672.875–5696.625 5722.875–5736.625 | Å | (C), Fe |
| Fe5782 | 5776.625–5796.625 | 5765.375–5775.375 5797.875–5811.625 | Å | Cr |
| Na D | 5876.875–5909.375 | 5860.625–5875.625 5922.125–5948.125 | Å | Na, C, (Mg) |
| TiO ₁ | 5936.625–5994.125 | 5816.625–5849.125 6038.625–6103.625 | mag | C |
| TiO ₂ | 6189.625–6272.125 | 6066.625–6141.625 6372.625–6415.125 | mag | C, V, Sc |

Metallicity Sensitive Absorption Features

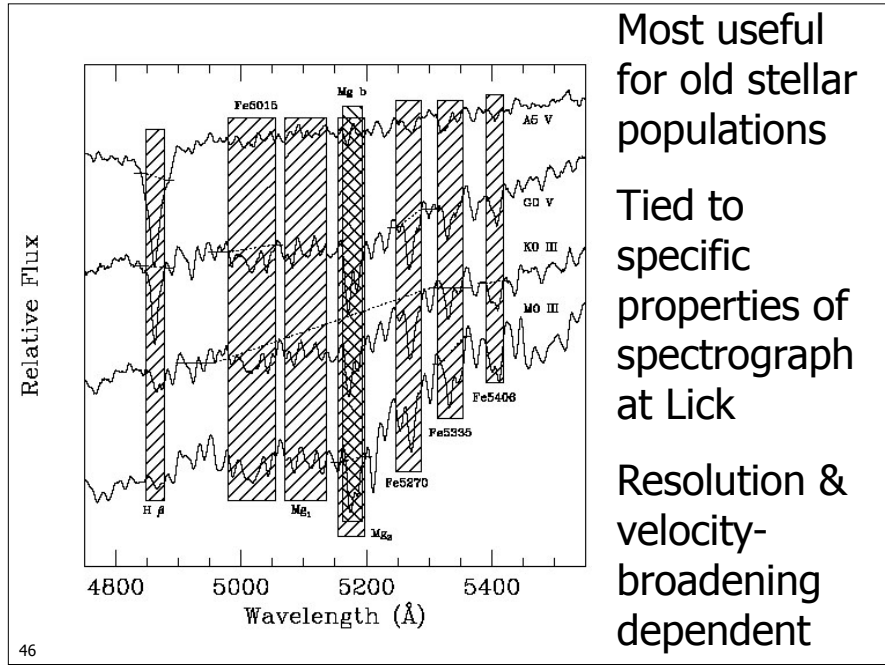
“Lick Indices”:

Characterize strength of optical absorption features

Age & Metallicity Sensitive

Note that the name sometimes has no connection to what elements are actually dominating the absorption!

Trager et al 1998



Lick indices are good probes of α -enhancement for unresolved galaxies

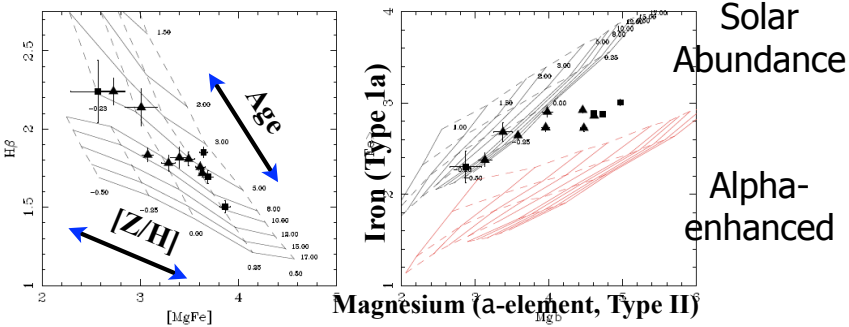


Figure 4. Stellar populations of Coma ETGs observed with LRIS in $(H\beta, [Mg/Fe])$ and $(Mg_b, (Fe))$ space, where $[Mg/Fe] = \sqrt{Mg_b \times (Fe)}$ and $(Fe) = (Fe5270 + Fe5335)/2$. Line strengths in this figure are measured through the synthesised 2'-diameter aperture. Triangles are S0's, squares are ellipses. Model grids come from the Cowley-Worley (1994) models, modified for $[Fe/Fe]$ as described in the §3.1. In both panels, solid lines are isochrones (constant age) and dashed lines are isofers (constant metallicity $[Z/H]$). In the left panel, the models are for $[Fe/Fe]$; models with higher $[Fe/Fe]$ have slightly lower $H\beta$ but similar $[Mg/Fe]$. Therefore this an appropriate grid from which to visually assess age and metallicity, although accurate determinations are made in $(H\beta, Mg_b, Fe5270, Fe5335)$ space (see text). In the right panel, grids have $[Fe/Fe] = 0, +0.3$ (upper and lower, respectively). This is an appropriate diagram from which to visually assess $[Fe/Fe]$.

Metallicity-sensitive indicators

Gas:
Tracks Z of current gas reservoir

Ratios of “strong” emission lines
Detailed fitting of weak+strong emission lines (like [OIII] “auroral” line; discussed in A541)

X-ray spectroscopy

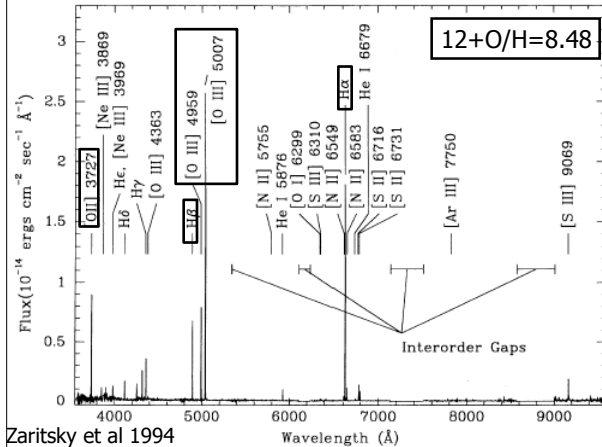
UV absorption spectroscopy (discussed in A541)

Most useful for old stellar populations

Tied to specific properties of spectrograph at Lick

Resolution & velocity-broadening dependent

Measuring gas-phase metallicity

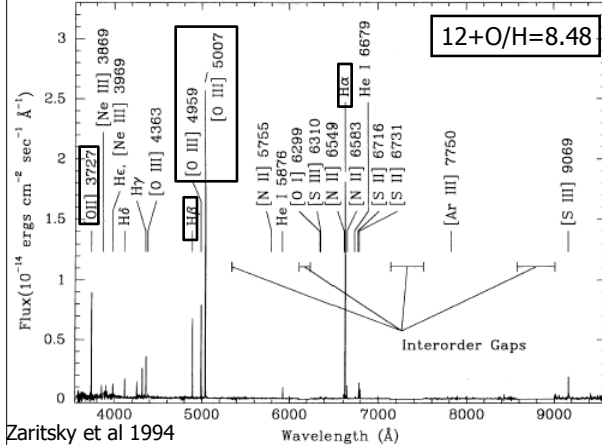


Need way of translating line ratios to elemental abundances.

Not as simple as taking ratio of O lines to H lines!

49

Measuring gas-phase metallicity



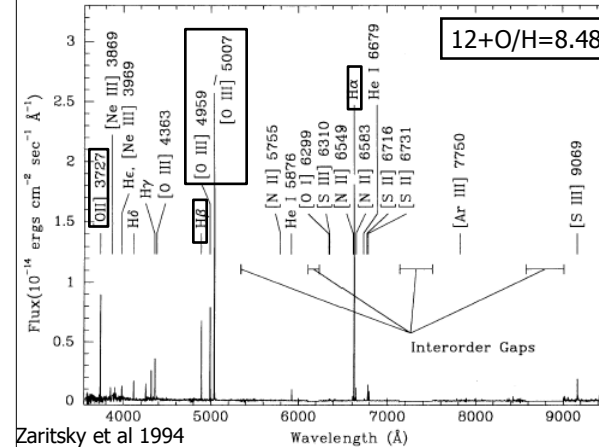
Hydrogen: recombination radiation

Line strength depends on n_e , Q_{ion} (electron density, ionizing flux).

Dependence on n_e , Q_{ion} often combined into an "ionization parameter" $U=n_\gamma/n_e$ where n_γ is # density of photons at Ly edge

51

Measuring gas-phase metallicity



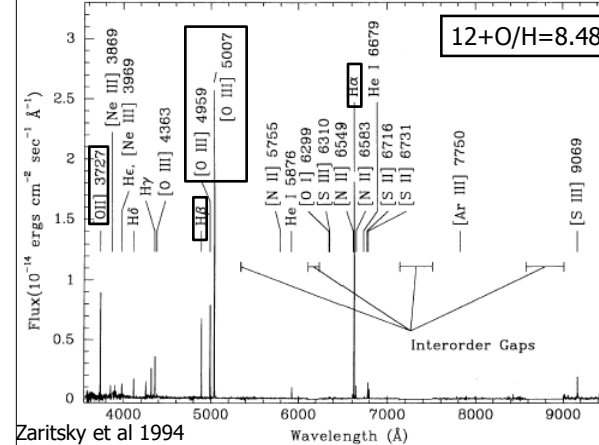
Hydrogen: recombination radiation

Oxygen: Collisionally excited forbidden lines

These are different physical processes. Their ratios don't immediately tell you much.

50

Measuring gas-phase metallicity



Oxygen: Collisionally* excited forbidden lines

Line strength depends on n_e , T_e (electron density, temperature)

Also will depend on degree of ionization, which also is affected by U

*Mostly. Some recombination contribution to [OII]3727Å

52

Example: Oxygen lines gets **stronger** in lower metallicity galaxies

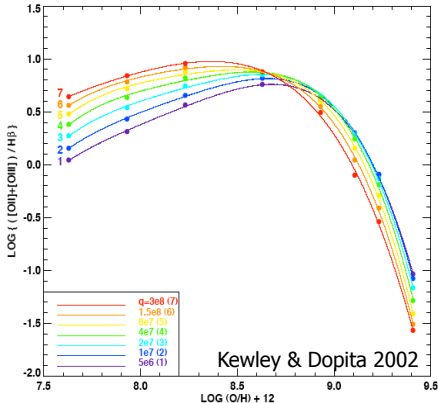
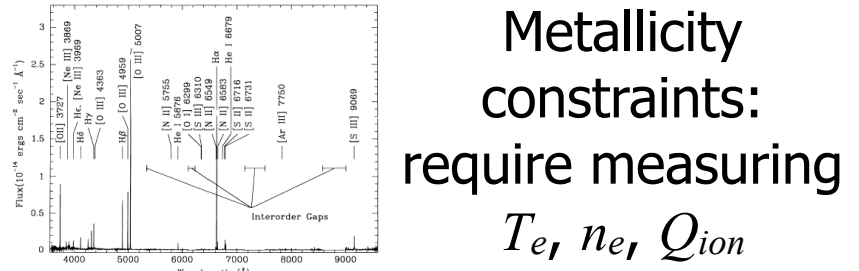


Fig. 4 -- The $\log([O\text{ II}] \lambda 3727 + [O\text{ III}] \lambda\lambda 4959, 5007/\text{H}\beta)$ (R_{23}) diagnostic for abundance versus metallicity. Curves for each ionization parameter between $q = 5 \times 10^6$ to $3 \times 10^8 \text{ cm/s}$ are shown. Filled circles represent the data points from our models at metallicities from left to right of 0.05, 0.1, 0.2, 0.5, 1.0, 1.5, 2.0, 3.0 Z_\odot . This figure is available in color from the on-line version of this article.

53

Fewer Metals = Less Cooling
Hotter Temp = Stronger O lines

- Metal lines are the principal coolants for the ISM
- When metals are absent, cooling is inefficient
- When cooling is inefficient, the ISM is hotter
- When the ISM is hotter, upper levels of higher ionization lines are more populated



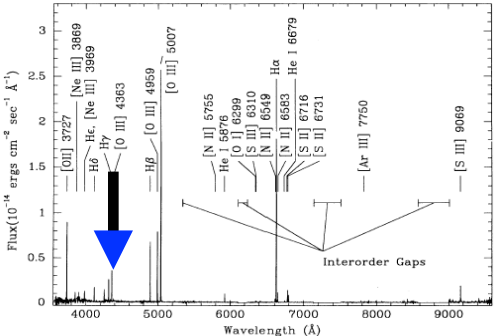
Q_{ion} : Constrain using photoionization models (usually constrains U instead)

n_e : Use “density sensitive” line ratios like $[\text{SII}]6716\text{\AA}, 6731\text{\AA}$, or $[\text{OII}]3727$ doublet

T_e : Use “temperature sensitive” line ratios like $[\text{OIII}]4363\text{\AA}, 5007\text{\AA}$

54

Difficulty measuring T_e with $[\text{OIII}]4363\text{\AA}$



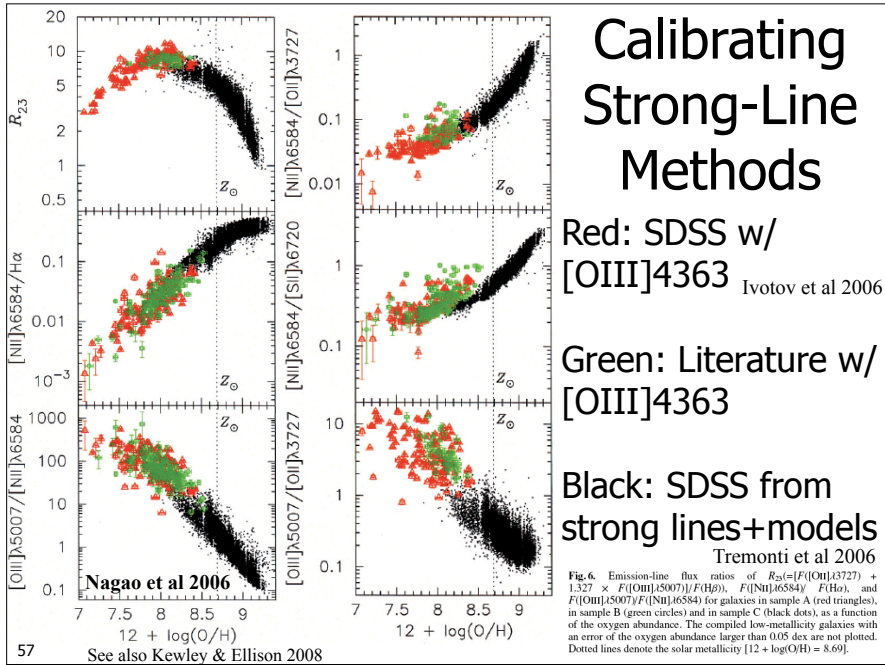
- This is a weak line! Needs high SNR
- Usual approach: Use “weak line” methods to calibrate techniques only using strong lines
- Or, use theoretical “grids” of line ratios as a function of U and Z .

“Strong Line Methods”

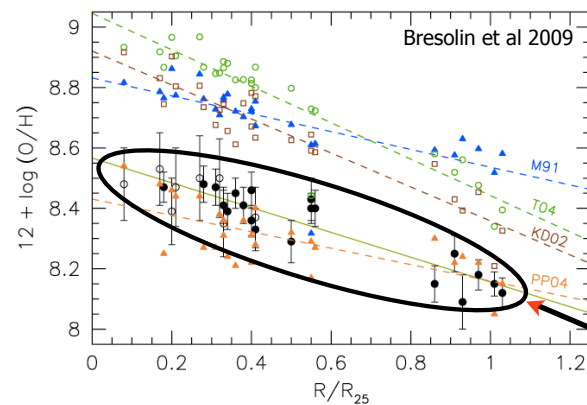
- “R23” method -- Uses $[\text{OII}], [\text{OIII}], \text{H}\beta$ lines
- Pilyugin P-Method -- like R23, but with empirical correction for ionization parameter
- “N2” -- $[\text{NII}]/\text{H}\alpha$
- “O3N2” -- $([\text{OIII}]/\text{H}\beta) / ([\text{NII}]/\text{H}\alpha)$
- “N2O2” -- $[\text{NII}]/[\text{OII}]$

Note: Should correct for stellar absorption lines, particular for Balmer lines

56



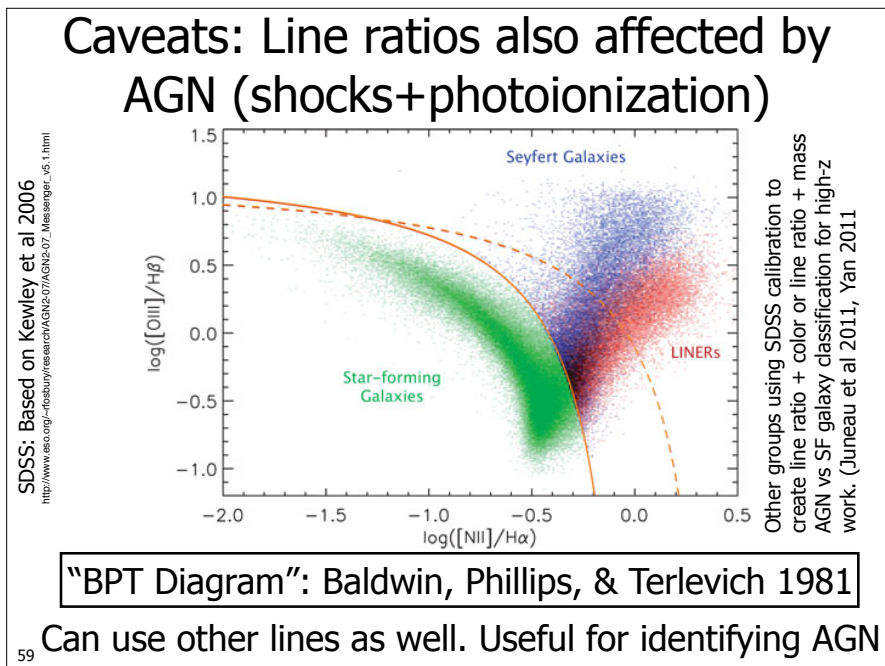
Calibrating Strong Line Methods:



Many common strong line indicators are biased high

Ground truth from stellar spectroscopy of young stars + weak line methods

Figure 12. Galactocentric distribution of the abundance values obtained from different strong-line methods and calibrations: R_{23} (McGaugh 1991: M91, blue triangles; Tremonti et al. 2004: T04, green circles), $[\text{N II}]/[\text{O II}]$ (Kewley & Dopita 2002: KD02, open squares), and N2 (Pettini & Pagel 2004: PP04, orange triangles). Linear least-squares fits are shown by the dashed lines, and labeled with the appropriate reference. The direct abundances determined from our work are shown by the full and open circle symbols, and the corresponding linear fit is shown by the continuous line (same as in Figure 10).



Basic Metallicity Results

Mass-metallicity correlation

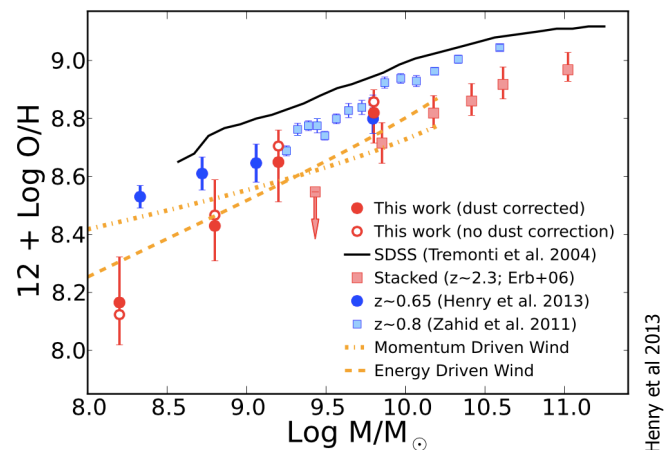
Evidence for mass dependent metal loss

Bulge vs disk metallicities

Metallicity gradients within disks

Metallicity and α -enhancement in ellipticals

Mass-Metallicity Evolves w/ Redshift



Fraught with peril, but would be surprised if it didn't evolve.

61

Example: Disk vs Bulge colors

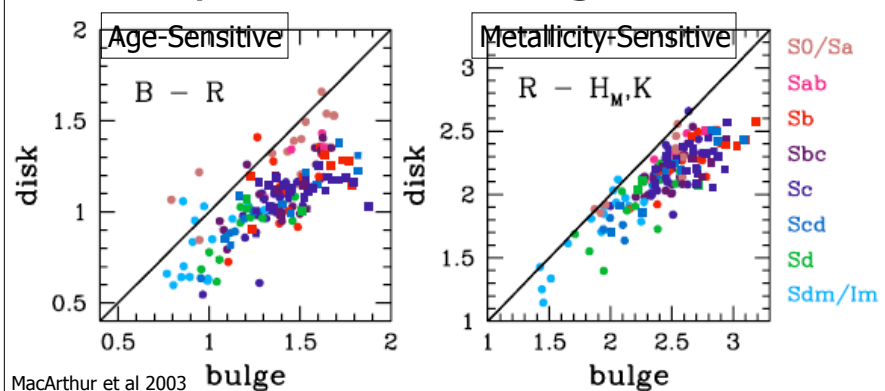
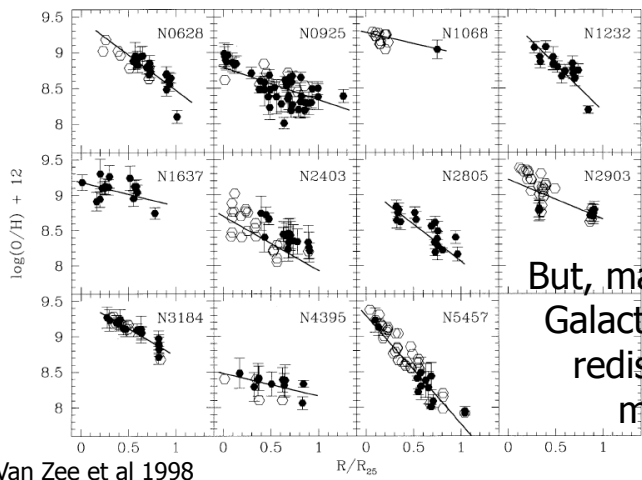


Fig. 8.—Disk colors (average of 1.5–2.5 disk scale length radial bin) as a function of bulge colors (average of 0.0–0.5 disk scale length radial bin). The solid horizontal lines represent a one-to-one mapping (for reference only). H_M is the “modified” H -band magnitude for the Courteau et al. sample, converted to K band with 2MASS $H-K$ colors (see text for details) for direct comparison with the K -band data of the Bj00 sample.

- Bulges are redder in B-R (older)
- Bulges are redder in R-K (more metal rich)

62

Within disks, metallicity gradients are common



Non-zero scatter at fixed radius, however.

But, many are flat.
Galactic fountain redistributing metals?

Van Zee et al 1998

Fig. 12.—Observed oxygen abundance gradients in all 11 spiral galaxies. The filled symbols represent HII regions from the present study. The open circles represent data from the literature: NGC 628 (McCall et al. 1989); NGC 925, Zaritsky et al. (1994); NGC 1068, Evans & Dopita (1987); Oey & Kennicutt (1993); NGC 2403, McCall et al. (1985); Fierro et al. (1986); Garnett et al. (1997); NGC 2903, McCall et al. (1985); Zaritsky et al. (1994); NGC 3184, Zaritsky et al. (1994); NGC 4395, McCall et al. (1985); NGC 5457, Kennicutt & Garnett (1996). The solid lines illustrate the derived oxygen abundance gradients.

Internal gradients w/ stars are weaker, and dominated by age

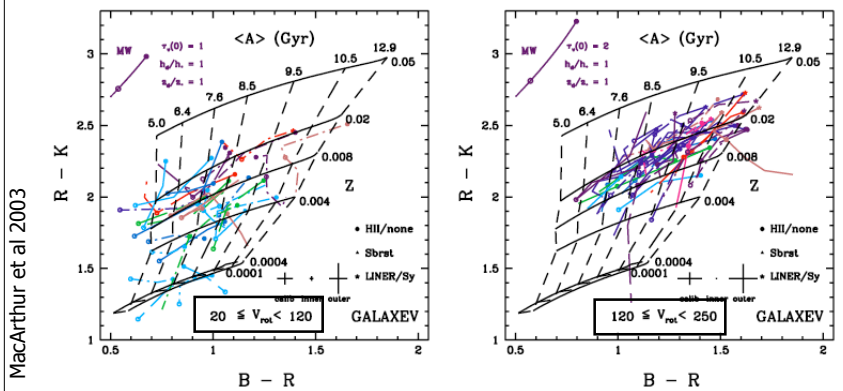
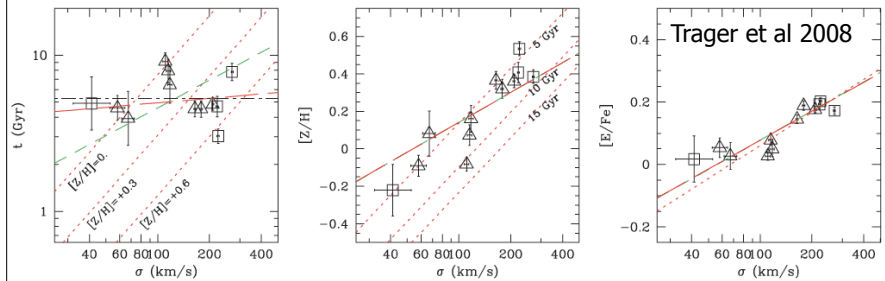


Fig. 11.—Near-IR-optical color-color plots separated by rotational velocity, V_{rot} (km s^{-1}), for the Bj00 sample. Galaxy center point types correspond to the level of nuclear activity in the galaxies (trends with colors and their gradients with nuclear activity were looked for but none were found, possibly because of small statistics).

Is this radial differences in metal loss? in gas accretion? in gas fraction?

64

Application: Ellipticals in Coma



More Massive Ellipticals have:

Higher metallicity

More alpha-enhancement

(No trend with age apparent, but luminosity weighted, so small "frosting" of SF at $z \sim 0.3$ could mask underlying age trend)